

Investigation into the Design of Ultra-Wideband (UWB) and Multi-band Antennas

Xiaoning Qiu




Faculty of Engineering
University of Technology, Sydney

**A Thesis Submitted for the degree of
Master of Engineering (Thesis)
June 2006**

Statement of Originality

I hereby declare that this thesis has not previously been submitted for a degree nor has it been submitted as part of requirements for a degree except as fully acknowledged within the text.

I also certify that the thesis presents my own work and has been written by me. Any help that I have received in my research work and the preparation of this thesis have been acknowledged. In addition, I certify that all information sources and literature used are indicated in the thesis

A handwritten signature in cursive script, reading "Qiu Xiaoning", written over a horizontal dashed line.

Xiaoning Qiu

Dedication

To my dear parents and relatives,
for their love and patience

Abstract

The rapid development of high speed wireless communications as well as other applications such as microwave imaging place extraordinary demands on spectrums for which ultra-wideband (UWB) and multi-band, e.g.: dual-band, techniques are useful. These UWB and multi-band services require UWB and multi-band antenna designs. Motivated by these applications, we first carried out the investigations on the family of square plate monopole (SPM) antennas for UWB applications. The family of square plate monopole (SPM) UWB antennas yields quite attractive features, viz.: ease of fabrication and freedom of dielectric material selection. Next, we considered the use of coplanar waveguide (CPW) fed printed UWB antenna for compact, body-worn applications. We investigated the antenna performance using empirical optimisation. The work on CPW-fed printed antennas has led to the development of multi-band antennas also.

For UWB antennas, we have first considered the modifications of well know square plate monopole (SPM) antennas. Our approach differs from other similar approaches on SPM antennas published in the literature. We have introduced symmetrical modifications to both bottom and top portions of the SPM antenna element. This has led

to the development of these types of symmetrically modified SPM antennas, viz.: symmetrically beveled SPM (SB-SPM) antenna, symmetrical semi-circular base SPM (SSCB-SPM) antenna and symmetrically notched SPM (SN-SPM) antenna. All these antennas have been empirically optimised using Feko[®] and the theoretical and experimental results are provided, in the point of view of reflection coefficient, radiation characteristics, phase response of antenna transfer function and time domain response.

For better suiting the compact and body-worn UWB applications, we have investigated the design of CPW-fed printed antenna. We have explored the antenna characteristics using empirical optimisation. The theoretical and experimental results for the completed CPW-fed printed antenna are provided, in the point of view of reflection coefficient, radiation characteristics, phase response of antenna transfer function, group delay and time domain response.

Lately, for multi-band antennas, we have investigated the design of multi-band printed antennas, which are fed by CPW, to suit emerging design requirements. Two CPW-fed dual-band printed antennas for GSM and DCS/PCS as well as DCS/PCS and IEEE 802.11b applications are proposed, which have C-shape and T-shape structures respectively. The theoretical and experimental results for these antennas are provided, in the point of view of reflection coefficient and radiation characteristics.

Due to the use of substrate material for the designs of UWB CPW-fed printed antenna as well as C-shaped and T-shaped dual-band CPW-fed printed antennas, the effects of substrate material tolerances on UWB characteristics and dual-band characteristics are investigated. Furthermore, as these UWB and dual-band CPW-fed printed antennas are

the promising candidates for wireless body-worn applications, which include wireless body area network (WBAN), the interactions between them and lossy material, such as human tissue, are investigated, which might help to decide the suitability of them for wireless body-worn applications.

Acknowledgments

A large number of people and organisations have assisted with this thesis written, which contains two years of research work. With all my respect to them, I would like to sincerely and gratefully thank them for their contributions to this thesis.

The first and most must be to thank my supervisor-Associate Professor Ananda Mohan Sanagavarapu (A. S. Mohan), who has shown his expert guidance, advice and knowledge so successfully in supervising his Master and Ph. D students in his research group. With his commitment and encouragement and training, I am able to improve and produce high quality research output during my research candidature, as well as my other group mates. I am so proud and pleasant to take this opportunity to appreciate him for these. Furthermore, the consolidation of my research work and the writing of this thesis and other technical papers during these years cannot be done successfully and smoothly without his efforts, which I want to show my appreciation to him again. Besides the efforts and help from my supervisor, I also need to thank my co-supervisor, Dr. K. K. Fung, who has delivered me lots of great help, advice and encouragement in consolidating my research work. At last, I need to thank Professor Hung T. Nguyen for his leadership in the research and development in Engineering Faculty at UTS.

I would also like to express my deep gratitude to my group mates and colleagues, who were in the past and some currently are the research students of my supervisor. These people are Dr. Andrew R. Weily, Dr. Heng-Mao (Hank) Chiu, Dr. Zhongwei (David) Tang, Dr. Kwok L. Chung and Mr. Tony Huang. The first person I mostly want to thank is Dr. Heng-Mao (Hank) Chiu. I earnestly appreciate his patience, intelligence and

sincere help and guidance at the early stage of my research work. It is really an honour to me to know this person. Dr. Zhongwei (David) Tang is not only a friend to me, but a mentor in many other aspects of my life. Dr. Kwok L. Chung influenced me much with his diligence and precision in every tiny piece of thing he does and encouraged me to pursue the best in my work. I really appreciate these above people who helped me to get trained to be a good researcher. It is such a pleasure for me to know and thank Dr. Andrew R. Weily for his enthusiastic help and support in using the Near-field Systems for antenna radiation patterns measurements. I value his friendly and intelligent advice. At last, I would like to give me appreciation to Mr Tony Huang, who is one of the most intelligent people I have met, especially in the field of software. During these two years, he has taught and helped me a lot, especially in programming and writing, although he often pretends not to be interested in anything to do with this field.

I am grateful to Rosa Tay, Mr. Ray Clout and Richard Turnell for their kind supports and technical help during my research candidature as well.

I would like to acknowledge that the work reported in this thesis is part of an Australian Research Council funded Discovery Project Grant: DP0346540 as well as a UTS internal Research Excellence Grant.

Table of Contents

ABSTRACT I

ACKNOWLEDGMENTS ERROR! BOOKMARK NOT DEFINED.

TABLE OF CONTENTS VI

LIST OF FIGURES IX

LIST OF TABLES XVIII

LIST OF ACRONYMS XX

1. Introduction and Overview 1

 1.1 INTRODUCTION TO ULTRA-WIDEBAND (UWB) WIRELESS SYSTEMS 1

 1.1.1 UWB for Short Range Indoor Wireless Communication Systems 4

 1.1.2 UWB for Microwave Imaging Systems 8

 1.2 REVIEW OF UWB ANTENNAS 9

 1.2.1 Differences between Traditional UWB and UWB Antennas 10

 1.2.2 Novel Three-Dimensional Antennas for UWB Applications 11

 1.2.3 Planar Antennas for UWB Applications 13

 1.3 INTRODUCTION TO MULTI-BAND WIRELESS COMMUNICATION SYSTEMS 15

 1.4 REVIEW OF MULTI-BAND ANTENNAS 16

 1.5 MOTIVATION FOR THE RESEARCH 17

 1.6 COMMON DESIGN OBJECTIVES OF UWB AND DUAL-BAND ANTENNAS 19

 1.7 ROAD MAP OF THIS THESIS 20

 1.8 PUBLICATIONS 21

2. Design of Square Plate Monopole Antennas with Symmetrical Modifications for Ultra-Wideband (UWB) Applications 23

 2.1 INTRODUCTION 23

2.2 DESIGN OBJECTIVES.....	26
2.3 EMPIRICAL MODELS OF PLATE MONOPOLE ANTENNAS	27
2.4 PROPOSED MODIFICATIONS ON SQUARE PLATE MONOPOLE (SPM) ANTENNAS	30
2.5 ANTENNA PERFORMANCE AND COMPARISON.....	34
2.5.1 <i>Input Reflection Coefficient</i>	35
2.5.2 <i>Impedance Bandwidth Comparison between Asymmetrical and Symmetrical Designs</i>	38
2.5.3 <i>Radiation Characteristics</i>	41
2.5.4 <i>Phase Response of Antenna Transfer Function</i>	45
2.5.5 <i>UWB Characteristics in Time Domain</i>	49
2.6 PARAMETRIC STUDIES	56
2.6 DISCUSSION.....	61
3. Coplanar-Waveguide-fed Compact Printed Antenna for Ultra-Wideband (UWB) Applications	62
3.1 INTRODUCTION.....	62
3.2 PROPOSED CPW-FED ANTENNA ELEMENT STRUCTURE	65
3.3 DESIGN PROCEDURE AND PROPOSED ANTENNA STRUCTURE	68
3.4 ANTENNA PERFORMANCE	93
3.5 DISCUSSION.....	95
4. Effects of Signal Dispersion, Material Tolerances and Lossy Material on Ultra-Wideband (UWB) Characteristics.....	97
4.1 INTRODUCTION.....	97
4.2 INFLUENCE OF SIGNAL DISPERSION ON UWB CHARACTERISTICS	98
4.2.1 <i>Phenomena of Signal Dispersion</i>	99
4.2.2 <i>Cause of Signal Dispersion</i>	100
4.2.3 <i>Phase Response of Antenna Transfer Function and Group Delay</i>	103
4.2.4 <i>UWB Characteristics in Time Domain</i>	109
4.3 UWB CHARACTERISTICS AGAINST DIELECTRIC MATERIAL TOLERANCES	114
4.4 UWB CHARACTERISTICS AGAINST LOSSY MATERIAL	116
4.5 DISCUSSION.....	124
5. C-Shaped and T-Shaped CPW-fed Antennas for Dual-Band Applications	126
5.1 INTRODUCTION.....	126
5.2 APPLICATIONS AND EMPIRICAL MODELS OF DUAL-BAND ANTENNAS	128
5.2.1 <i>Introducing Dual-Band and Multi-Band Wireless Applications</i>	128

5.2.2 Empirical Model of a Dual-Band Antenna	129
5.3 PROPOSED DUAL-BAND ANTENNA STRUCTURES	131
5.3.1 Proposed Structure of C-Shaped CPW-fed Printed Antenna.....	131
5.3.2 Parametric Studies of C-Shaped CPW-fed Printed Antenna	134
5.3.3 Proposed Structure of T-Shaped CPW-fed Printed Antenna	138
5.3.4 Parametric Studies of T-Shaped CPW-fed Printed Antenna.....	140
5.4 PERFORMANCE OF PROPOSED DUAL-BAND ANTENNAS	145
5.4.1 Performance of C-Shaped CPW-fed Printed Antenna	145
5.4.2 Performance of T-Shaped CPW-fed Printed Antenna	148
5.5 DUAL-BAND CHARACTERISTICS AGAINST DIELECTRIC MATERIAL TOLERANCES AND LOSSY MATERIAL.....	151
5.5.1 Dual-Band Characteristics against Dielectric Material Tolerances....	151
5.5.2 Dual-Band Characteristics against Lossy Material	153
5.6 DISCUSSION.....	160
6. Conclusion.....	162
6.1 MAJOR CONTRIBUTION OF THIS THESIS.....	162
6.1.1 Introduction.....	162
6.1.2 The Major Contribution	163
6.2 SUGGESTED IMPROVEMENTS AND FUTURE WORK	167
REFERENCE.....	168
APPENDIX- A.....	178
NSI TM NEAR-FIELD 700S-50 SPHERICAL SYSTEM	178
APPENDIX- B	184
DATA FOR CALCULATED TIME DOMAIN RESPONSE	184
B.1 Symmetrically Modified Square Plate Monopole (SPM) Antennas.....	185
B.1.1 Symmetrically Beveled Square Plate Monopole (SB-SPM) Antenna ...	185
B.1.2 Symmetrically Semi-Circular Base Square Plate Monopole (SSCB-SPM) Antenna	191
B.1.3 Symmetrically Notched Square Plate Monopole (SN-SPM) Antenna ..	197
B.2 Printed CPW-fed UWB Antenna.....	203

List of Figures

Fig. 1.1 EIRP criteria for indoor and outdoor UWB applications	3
Fig. 1.2 The phase response comparison between cavity-backed Archimedean spiral (CBAS) antenna and TEM horn antenna	11
Fig. 2.1 Techniques to improve the impedance bandwidth of SPM antennas: (a) the use of bevelling technique; (b) use of semi-circular base plate shape; (c) single-sided bevelling combined with short-circuiting pin; (d) the use of double-feed; (e) introduction of notches at the bottom portion of antenna element; (f) asymmetrical feed arrangement	25
Fig. 2.2 (a) Square plate monopole (SPM) antenna, (b) Comparison between the measured and simulated results of the SPM antenna	28
Fig. 2.3 Reflection coefficients of antennas listed in Table 2.1	29
Fig. 2.4 Comparison of reflection coefficients between different dimensions of SPM antenna	30
Fig. 2.5 Schematic diagrams of a family of asymmetrically and symmetrically modified SPM antennas: (a) asymmetrically beveled SPM (ASB-SPM) antenna; (b) symmetrically beveled SPM (SB-SPM) antenna; (c) asymmetrically semi-circular base SPM (ASSCB-SPM) antenna; (d) symmetrically semi-circular base SPM (SSCB-SPM) antenna; (e) asymmetrically notched SPM (ASN-SPM) antenna; (f) symmetrically notched SPM (SN-SPM) antenna.....	32
Fig. 2.6 Current distributions of symmetrically modified SPM antennas and their corresponding asymmetrical counterparts at spot frequency of 6GHz. (a) symmetrically (SB-SPM) and asymmetrically (ASB-SPM) beveled SPM antennas, (b) symmetrically (SSCB-SPM) and asymmetrically (ASSCB-SPM) semi-circular base SPM antennas and (c) symmetrically (SN-SPM) and asymmetrically (ASN-SPM) notched SPM antennas.....	33

Fig. 2.7 Prototypes of the symmetrically modified SPM antennas: (a) SB-SPM antenna and (b) SSCB-SPM antenna (Continued in next page).....	34
Fig. 2.7 (Continued from last page) Prototypes of the symmetrically modified SPM antennas: (c) SN-SPM antenna	35
Fig. 2.8 Reflection coefficient comparisons between asymmetrically and symmetrically modified SPM antennas (a) SB-SPM and ASB-SPM antennas; (b) SSCB-SPM and ASSCB-SPM antennas (Continued in next page).....	36
Fig. 2.8 (Continued from last page) Reflection coefficient comparisons between asymmetrically and symmetrically modified SPM antennas (c) SN-SPM and ASN-SPM antennas.....	37
Fig. 2.9 (a) Bandwidth below -10dB comparison between SB-SPM and ASB-SPM antennas with BW = 15mm and BH varying from 1mm to 15mm. (b) Percentage bandwidth below -15dB comparison of SB-SPM antenna between BH = 6, 7, 8 and 9mm with BW varying from 1mm to 15mm. (c) Bandwidth below -10dB comparison between SB-SPM and ASB-SPM antennas with BH = 7mm and BW varying from 1mm to 15mm. (d) Bandwidth comparison of impedance bandwidth lower than -15dB in UWB band (3.1GHz-10.6GHz) between SB-SPM and ASB-SPM antennas with BH = 7mm and BW varying from 1mm to 15mm.....	39
Fig. 2.10 (a) Bandwidth below -10dB comparison between SSCB-SPM and ASSCB-SPM antennas with R varying from 1 to 15mm, (b) Percentage bandwidth below -15dB comparison between SSCB-SPM and ASSCB-SPM antennas with R varying from 1 to 15mm.....	40
Fig. 2.11 (a) Bandwidth below -10dB comparison between SN-SPM and ASN-SPM antennas with NW = 7mm and NH varying from 1mm to 14mm. (b) Bandwidth below -10dB comparison between SN-SPM and ASN-SPM antennas with NH = 3mm and NW varying from 1mm to 14mm.....	41
Fig. 2.12 (a) Coefficient of omni-directionality vs. frequency of SB-SPM antenna (Fig. 2.7 (a)); (b) <i>xy</i> -plane normalised radiation patterns of SB-SPM antenna at spot frequency 4.5GHz; (c) <i>xy</i> -plane normalised radiation patterns of SB-SPM antenna at spot frequency 7.5GHz and (d) <i>xy</i> -plane normalised radiation patterns of SB-SPM antenna at spot frequency 10.5GHz	42
Fig. 2.13 (a) Coefficient of omni-directionality vs. frequency of SSCB-SPM antenna (Fig. 2.7 (b)); (b) <i>xy</i> -plane normalised radiation patterns of SSCB-SPM antenna at spot frequency 4.5GHz; (c) <i>xy</i> -plane normalised radiation patterns of SSCB-SPM antenna at spot frequency 7.5GHz and (d) <i>xy</i> -plane normalised radiation patterns of SSCB-SPM antenna at spot frequency 10.5GHz	43
Fig. 2.14 (a) Coefficient of omni-directionality vs. frequency of SN-SPM antenna (Fig. 2.7 (c)); (b) <i>xy</i> -plane normalised radiation patterns of SN-SPM antenna at spot frequency 4.5GHz; (c) <i>xy</i> -plane normalised radiation patterns of SN-SPM antenna at spot frequency 7.5GHz and (d) <i>xy</i> -plane normalised radiation patterns of SN-SPM antenna at spot frequency 10.5GHz	44

- Fig. 2.15** The antenna positioning schemes for a link in 3-D schematic diagrams on separate ground planes and a single ground plane: (a) Face to face; (b) Side by side and (c) Face to side. For simplicity, square plate monopole (SPM) antenna is used in these schematic diagrams.....46
- Fig. 2.16** Phase response of SB-SPM antenna for configurations shown in Figs. 2.15..47
- Fig. 2.17** Phase response of the SSCB-SPM antenna for configurations shown in Figs. 2.15 (Continued in next page).....47
- Fig. 2.17** (Continued from last page) Phase response of the SSCB-SPM antenna for configurations shown in Figs. 2.1548
- Fig. 2.18** Phase response of the SN-SPM antenna for configurations shown in Figs. 2.1548
- Fig. 2.19** (a) Waveform of input pulse and (b) power spectral density of the input pulse normalised to the FCC indoor and out door EIRP masks.50
- Fig. 2.20** Analytical model of system configuration with a pair of antennas for the theoretical investigations of UWB time-domain characteristics.....50
- Fig. 2.21** (Continued from last page) Normalised received waveforms of UWB pulses for the SB-SPM antenna for configurations shown in Figs. 2.15. The dotted waveforms at the left indicate the normalised transmitted UWB pulse.....53
- Fig. 2.22** Normalised received waveforms of UWB pulses for the SSCB-SPM antenna for configurations shown in Figs. 2.15. The dotted waveforms at the left indicate the normalised transmitted UWB pulse.53
- Fig. 2.23** Normalised received waveforms of UWB pulses for the SN-SPM antenna for configurations shown in Figs. 2.15. The dotted waveforms at the left indicate the normalised transmitted UWB pulse.54
- Fig. 2.24** Bandwidth comparison of SB-SPM antenna with dimension schemes shown in **Beveled** column of Table 2.4. Subscripts “B” and “T” stand for bottom and top respectively. (Continued in next page).....57
- Fig. 2.24** (Continued from last page) Bandwidth comparison of SB-SPM antenna with dimension schemes shown in **Beveled** column of Table 2.4. Subscripts “B” and “T” stand for bottom and top respectively.58
- Fig. 2.25** Bandwidth comparison of SSCB-SPM antenna with dimension schemes shown in **Semi-Circular Base** column of Table 2.4. Subscripts “B” and “T” stand for bottom and top respectively.58
- Fig. 2.26** Bandwidth comparison of SN-SPM antenna with dimension schemes shown in **Notched** column of Table 2.4. Subscripts “B” and “T” stand for bottom and top respectively.59

- Fig. 3.1** The initial prototype of the antenna which formed basis for improvement66
- Fig. 3.2** (a) Electric field and (b) Magnetic field on the cross-section plane of CPW at spot frequency of 5.5GHz67
- Fig. 3.3** (a) Distributions of magnetic field and (b) electric field on prototype antenna at spot frequency of 5.5GHz67
- Fig. 3.4** (a) Schematic diagram of the coplanar waveguide, (b) Side view of the proposed CPW-fed antenna element shown in Fig 3.169
- Fig. 3.5** (a) Comparison of centre conductor width of CPW versus its slot width with $h = 1.524\text{mm}$, $Z_0 = 50\Omega$ and $\epsilon_r = 2.2, 3.38, 4.4, 6.15$ and 10.2 ; (b) Comparison of centre conductor width of CPW versus its slot width with $\epsilon_r = 3.38$, $Z_0 = 50\Omega$ and $h = 0.508\text{mm}, 0.813\text{mm}$ and 1.524mm 71
- Fig. 3.6** Input characteristic impedance of coplanar waveguide with dimensions of $\epsilon_r = 3.38$, $h = 1.524\text{mm}$, $W_f = 5.5\text{mm}$ and $g = 0.3\text{mm}$ 72
- Fig. 3.7** Antenna geometries with single-notched-step (SNS) modifications investigated in *Step 3 a)*: (a) modifications applied only at bottom; (b) modifications applied only at top; (c) modifications applied at both bottom and top of the horizontal slots73
- Fig. 3.8** Comparison of reflection coefficients for SNS modifications applied only at bottom, only at top and at both bottom and top of the horizontal slots. The dimensions of SNS modifications are (a) $NW = 6\text{mm}$ and $NH = 2\text{mm}$ and (b) $NW = 6\text{mm}$ and $NH = 3\text{mm}$74
- Fig. 3.9** General antenna geometry with SNS modifications investigated in *Step 3 b)*..75
- Fig. 3.10** A designation method for categorising the cases in investigations76
- Fig. 3.11** Comparison of reflection coefficients between VMOB and VMOT for: (a) *w-five-two-three* cases; (b) *h-two-six-five* cases; (c) *w-six-two-three* cases; (d) *h-three-six-five* cases; (e) *w-seven-three-four* cases; (f) *h-four-seven-six* cases81
- Fig. 3.12** Comparison of reflection coefficients between different variables: (a) *w-five-three-four* cases; (b) *h-four-five-six* cases; (c) *w-six-two-three* cases; and (d) *h-three-six-six* cases.....82
- Fig. 3.13** Comparison of reflection coefficients between different sub-classes: (a) *w-six-* cases and (b) *h-three-* cases.....83
- Fig. 3.14** Enlarged illustration of the centre portion of the antennas studied in *Step 4* ..84
- Fig. 3.15** Comparison of reflection coefficients for antennas studied in *Step 4*, between different gap widths.....85

- Fig. 3.16** (a) Illustration of antenna configuration after introducing symmetrical SNS modifications; (b) Antenna configuration with further symmetrical SNS modifications; (c) Antenna configuration with further symmetrical SBS modifications.....86
- Fig. 3.17** Comparison of reflection coefficients between further symmetrical SNS and SBS modifications: (a) $NH = BH = 1.5\text{mm}$, $NW = BW = 3\text{mm}$; (b) $NH = BH = 2\text{mm}$, $NW = BW = 4\text{mm}$88
- Fig. 3.18** Comparison of reflection coefficients between different BW for further symmetrical SBS modifications when $BH = 1.5\text{mm}$88
- Fig. 3.19** (a) Comparison of reflection coefficients between different L1; (b) Comparison of xy-plane normalised co-polarization component at 8.5GHz between different L189
- Fig. 3.20** (a) Comparison of reflection coefficients between different L2; (b) Comparison of xy-plane normalised co-polarization component at 8.5GHz between different L290
- Fig. 3.21** (a) The geometry and (b) prototype of the compact printed CPW-fed UWB antenna92
- Fig. 3.22** The simulated and measured reflection coefficients of the proposed printed CPW-fed UWB antennas93
- Fig. 3.23** The coefficient of omni-directionality vs. frequency of the compact printed CPW-fed antenna94
- Fig. 3.24** xy-plane normalised radiation patterns of the compact printed CPW-fed antenna at (a) 4.5GHz, (b) 6.5GHz, (c) 8.5GHz and (d) 10.5GHz.95
- Fig. 4.1** Hypothetical antenna model for theoretical modelling of signal dispersion: (a) front view and (b) top view.....101
- Fig. 4.2** The antenna positioning schemes for a link in 3-D schematic diagrams. (a) Face-to-face with substrates facing each other, (b) Narrow sides of substrate facing each other with antennas looking at identical direction (Continued in next page)105
- Fig. 4.2** (Continued from last page) The antenna positioning schemes for a link in 3-D schematic diagrams. (c) Face-to-face with antennas facing each other, (d) Narrow sides of substrate facing each other but antennas looking at opposite directions, (e) Narrow side of one substrate facing antenna of the other one forming a T-section, (f) Narrow side of one substrate facing the wide substrate side of the other one forming a T-section and (g) Antenna side of one facing the wide substrate side of the other one. The black and grey areas indicate the copper and substrate of the printed antenna.106
- Fig. 4.3** The phase response of the compact printed antenna in the antenna positioning schemes shown in Fig. 4.2 (a) Face-to-face with substrates facing each other, (b)

Narrow sides of substrate facing each other with antennas looking at identical direction, (c) Face-to-face with antennas facing each other, (d) Narrow sides of substrate facing each other but antennas looking at opposite directions, (e) Narrow side of one substrate facing antenna of the other one forming a T-section, (f) Narrow side of one substrate facing the wide substrate side of the other one forming a T-section. (Continued in next page) 107

Fig. 4.3 (Continued from last page) The phase response of the compact printed antenna in the antenna positioning schemes shown in Fig. 4.2 (g) Antenna side of one facing the wide substrate side of the other one. 108

Fig. 4.4 The group delays of compact printed antennas in the antenna positioning schemes shown in Fig. 4.2. 108

Fig. 4.5 (a) Waveform of input pulse and (b) power spectral density of the input pulse normalised to the FCC indoor and out door EIRP masks. 110

Fig. 4.6 Normalised received waveforms of UWB pulses for the compact CPW-fed printed antenna in the antenna positioning schemes shown in Figs. 4.2 (a) Substrate face substrate, (b) Side by side with coppers facing identical, (c) Copper face copper, (d) Side by side with copper facing opposite, (e) T-shaped relative position with one copper side facing inwards and (f) T-shaped relative position with one copper side facing outwards. The dotted waveforms at the left indicate the normalised transmitted waveform of UWB pulse. (Continued in next page)..... 111

Fig. 4.6 (Continued from last page) Normalised received waveforms of UWB pulses for the compact CPW-fed printed antenna in the antenna positioning schemes shown in Figs. 4.2 (g) Copper side of one antenna facing the substrate side of the other one antenna. The dotted waveforms at the left indicate the normalised transmitted waveform of UWB pulse. 112

Fig. 4.7 The variation of reflection coefficients for the UWB CPW-fed printed antenna due to dielectric constant and thickness tolerances on substrate RO4003CTM in four extreme-case scenarios..... 115

Fig. 4.8 The variation of coefficients of omni-directionality vs. frequency for the UWB CPW-fed printed antenna due to dielectric and constant thickness tolerances on Rogers[®] RO4003CTM in four extreme-case scenarios 116

Fig. 4.9 (a) Geometry of the printed CPW-fed UWB antenna, the units are in mm; (b) Side view and top view of a lossy circular cylinder placed close to the antenna. 118

Fig. 4.10 Reflection coefficients of UWB printed antenna close to a lossy cylinder with spacing $D = 2, 8, 15$ and 25mm 119

Fig. 4.11 Normalised radiation patterns at spot frequency 4.5GHz: (a) $D = 2\text{ mm}$, (b) $D = 8\text{mm}$. (c) $D = 15\text{ mm}$ and (d) $D = 25\text{mm}$ 119

Fig. 4.12 (a) Front-to-back ratio and (b) front-to-side ratio of co-polarization component of radiation patterns for the printed antenna in the presence of lossy cylinder for different spacing $D = 2, 8$ and 25mm 120

Fig. 4.13 Power absorbed of 1g lossy material due to the UWB CPW-fed printed antenna with spacing $D = 15\text{mm}$: (a) 4.5GHz ; (b) 6.5GHz ; (c) 8.5GHz and (d) 10.5GHz 122

Fig. 4.14 Power absorbed of 10g lossy material due to the UWB CPW-fed printed antenna with spacing $D = 15\text{mm}$: (a) 4.5GHz ; (b) 6.5GHz ; (c) 8.5GHz and (d) 10.5GHz 123

Fig. 5.1 Empirical model of dual-band antenna, (a) monopole antennas and (b) idea behind dual-band antenna 130

Fig. 5.2 Proposed structure of the dual-band C-shaped CPW-fed printed antenna (unit: mm) 132

Fig. 5.3 Current distributions of dual-band C-shaped CPW-fed printed antenna with identical scale: (a) 0.9GHz , (b) 1.8GHz and (c) 2.65GHz 134

Fig. 5.4 The comparison of simulated reflection coefficients of proposed dual-band C-shaped CPW-fed printed antenna with gap distance (the distance between the bottom of the C-shaped element and the ground plane) of $7, 10, 13$, and 16mm respectively 135

Fig. 5.5 The comparison of simulated reflection coefficients of proposed dual-band C-shaped CPW-fed printed antenna with gap distance (the gap distance of the mouth of the C-shaped element) of $2, 3$, and 4mm respectively..... 135

Fig. 5.6 The comparison of simulated reflection coefficients of proposed dual-band C-shaped CPW-fed printed antenna with different (a) widths and (b) heights of the ground planes 137

Fig. 5.7 Proposed structure of the dual-band T-shaped CPW-fed printed antenna (unit: mm) 138

Fig. 5.8 Current distributions of printed dual-band T-shaped CPW-fed antenna with identical scale: (a) 1.85GHz and (b) 2.4GHz 139

Fig. 5.9 The schematic diagram for the investigation on the effect of the length of the horizontal strip of the L-shaped element for the proposed T-shaped antenna 141

Fig. 5.10 The comparison of simulated reflection coefficients of proposed dual-band T-shaped CPW-fed printed antenna, studied in Fig. 5.15, with lengths of $-3.5, 0, 3, 6.5, 10.5, 14.5$ and 18.5mm for the horizontal strip of L-shaped element. ⁽¹⁾ The minus value represents the short-circuited L-shape element residing at the right side of the vertical strip of the T-shaped element. ⁽²⁾ Zero represents that no short circuiting L-shaped element is used..... 141

- Fig. 5.11** The comparison of simulated reflection coefficient of proposed dual-band T-shaped CPW-fed printed antenna with lengths of 0, 2.5 and 4.5mm for the bent portion of T-shaped element longer arm..... 143
- Fig. 5.12** The comparison of simulated reflection coefficient of proposed dual-band T-shaped CPW-fed antenna with different widths for ground plane: (a) left ground plane and (b) right ground plane 144
- Fig. 5.13** The comparison of simulated reflection coefficient of proposed dual-band T-shaped CPW-fed antenna with different heights for ground plane 145
- Fig. 5.14** (a) Dimensions and (b) prototype of the proposed dual-band C-shaped CPW-fed printed antenna..... 146
- Fig. 5.15** The simulated and measured reflection coefficients of the proposed dual-band C-shaped CPW-fed printed antenna..... 146
- Fig. 5.16** Normalised radiation patterns of the proposed dual-band C-shape CPW-fed printed antenna at xy -, xz - and yz -planes: (a) simulated results at 0.9GHz and (b) measured and simulated results at 1.8GHz. 147
- Fig. 5.17** (a) Dimensions and (b) prototype of the proposed printed dual-band T-shaped CPW-fed antenna 149
- Fig. 5.18** The simulated and measured reflection coefficient of the proposed printed dual-band T-shaped CPW-fed antenna 149
- Fig. 5.19** Measured and simulated normalised radiation patterns of the proposed T-shape CPW-fed printed antenna at xy -, xz - and yz -planes: (a) at 1.85GHz and (b) at 2.5GHz 150
- Fig. 5.20** The variations of reflection coefficients for the dual-band C-shaped CPW-fed printed antenna due to thickness and dielectric constant tolerances of Rogers® RO4003CTM in four extreme-case scenarios..... 152
- Fig. 5.21** The variations of reflection coefficients for the dual-band T-shaped CPW-fed printed antenna due to thickness and dielectric constant tolerances of Rogers® RO4003CTM in four extreme-case scenarios..... 153
- Fig. 5.22** Side view and top view of a lossy circular cylinder placed close to the proposed antenna element. 154
- Fig. 5.23** Comparison of reflection coefficients of CPW-fed printed antennas lose to a lossy cylinder with spacing $D = 2, 8, 15$ and 25mm (a) C-shaped printed antennas and (b) T-shaped printed antennas 155
- Fig. 5.24** Radiation patterns of C-shaped CPW-fed printed antenna with spacing $D = 2\text{mm}$ and 15mm to the lossy cylinder at resonant frequencies: (a) 0.9GHz and (b) 1.8GHz. 156

Fig. 5.25 Radiation patterns of T-shaped CPW-fed printed antenna with spacing $D = 2\text{mm}$ and 15mm to the lossy cylinder at resonant frequencies: (a) 1.85GHz and (b) 2.5GHz 157

Fig. 5.26 Power absorbed of 1g and 10g lossy material due to the dual-band C-shaped CPW-fed printed antenna with spacing $D = 15\text{mm}$: (a) 0.9GHz and (b) 1.8GHz 158

Fig. 5.27 Power absorbed of 1g and 10g lossy material due to the dual-band T-shaped CPW-fed printed antenna with spacing $D = 15\text{mm}$: (a) 1.85GHz and (b) 2.5GHz 159

Fig. A.1 Antenna measurement conducted by the author inside the anechoic chamber at CSIRO ICT centre. Photo courtesy of Dr. Andrew Weily of Macquarie University, NSW, Australia 180

List of Tables

Table 2.1 Summary of dimensions and configurations of antennas studied	29
Table 2.2 Summary of coefficient of omni-directionality for the symmetrically modified SPM antennas at spot frequencies chosen and percentage of omni-directional radiation characteristics in UWB band	44
Table 2.3 Summary of fidelity factor between the transmitting and receiving UWB pulses for the family of symmetrically modified SPM antennas for the configurations shown Fig. 2.15.....	56
Table 2.4 Summary of dimensions for the fixed bottom modifications. Subscript “B” stands for bottom.....	57
Table 2.5 Summary of dimensions for the top modifications. Subscript “T” stands for top.....	57
Table 3.1 Summary of cases investigated for the influence of WIDTH of SNS modifications applied at the bottom and at the top of the horizontal slots on antenna impedance matching performance	77
Table 3.2 Summary of cases investigated for the influence of height of SNS modifications applied at the bottom and at the top of the horizontal slots on antenna impedance matching performance	78
Table 3.3 Summary of five examples in illustrating the three fixed dimensional parameters and the variable for a given class of cases.....	79
Table 3.4 Summary of particular values for the variables of antennas with different level of modifications that are shown in Fig. 3.13. When the variables of antennas with different levels of modifications increase beyond these particular values, the impedance bandwidth will be narrowed down.....	83
Table 3.5 Summary of variables for the completed printed CPW-fed UWB antenna shown in Fig. 3.21 (a)	92

Table 4.1 Summary of fidelity factor between the transmitting and receiving UWB pulses for the CPW-fed printed antenna in the antenna positioning schemes of Fig. 4.2..... 113

Table 4.2 Summary of the RO4003C™ substrate materials used in the UWB CPW-fed printed antenna..... 114

Table 4.3 Maximum average 1g SAR (W/Kg, Input Power: 1W) 122

Table 4.4 Maximum average 10g SAR (W/Kg, Input Power: 1W) 123

Table 5.1 Summary of spectrums for different mobile cellular and wireless LAN applications 129

Table 5.2 Summary of parameters and performance illustrated in Fig. 5.10 for the proposed dual-band T-shaped CPW-fed printed antenna. The bandwidths are defined as the -10dB reflection coefficient bandwidth. 142

Table 5.3 Summary of the substrate materials used in the Design Example 151

Table 5.4 Maximum average 1g and 10g SAR of the printed dual-band C-shaped CPW-fed antenna (W/Kg, Input Power: 1W) 158

Table 5.5 Maximum average 1g and 10g SAR of printed dual-band T-shaped CPW-fed antenna (W/Kg, Input Power: 1W) 159

List of Acronyms

ASB-SPM	Asymmetrically Beveled Square Plate Monopole
ASN-SPM	Asymmetrically Notched Square Plate Monopole
ASSCB-SPM	Asymmetrically Semi-Circular Base Square Plate Monopole
BW	Bandwidth
CBAS	Cavity-Backed Archimedean Spiral
CDMA	Code Division Multiple Access
CPW	Coplanar Waveguide
CSL	Coupled Slotline
DRA	Dielectric Resonator Antenna
DCS	Digital Cellular System
EIRP	Equivalent Isotropic Radiated Power
FCC	Federal Communication Committee
Feko	<i>FEldberechnung bei Körpern mit beliebiger Oberfläche</i>
FSS	Frequency Selective Surface
GA	Genetic Algorithm
GSM	Group Spéciale Mobile
GPRS	General Packet Radio Service
GPS	Global Positioning System
HFSS	High Frequency Structure Simulator
HiperLan/x	Standards for Radio Local Area Network
HOM	Higher Order Mode
IEEE 802.11a/b/g	Standards for Wireless Local Area Networks (WLAN)
IRA	Impulse Radiating Antennas

LTCC	Low Temperature Cofired Ceramic
LOS	Line of Sight
MB	Megabyte
MoM	Methods of Moments
NMT	Nordic Mobile Telephone
NSI	Near-field System Inc.
OBS	One Beveled Step
ONS	One Notched Step
PCB	Printed Circuit Board
PCS	Personal Communication Services
RF	Radio Frequency
SAR	Specific Absorption Rate
SB-SPM	Symmetrically Beveled Square Plate Monopole
SMA	SubMiniature Version A
SN-SPM	Symmetrically Notched Square Plate Monopole
SPM	Square Plate Monopole
SSCB-SPM	Symmetrically Semi-Circular Base Square Plate Monopole
TEM	Transverse Electromagnetic
UMTS	Universal Mobile Telecommunications Systems
UWB	Ultra Wideband
WBAN	Wireless Body Area Network
WLAN	Wireless Local Area Network
WPAN	Wireless Personal Area Network